

RESEARCH ARTICLE

Integral Adaptive Sliding Mode Control for Quadcopter UAV Under Variable Payload and Disturbance

AHMED ELTAYEB¹, MOHD FUA'AD RAHMAT¹, (Senior Member, IEEE),
MOHD ARIFFANAN MOHD BASRI¹, M. A. MOHAMMED ELTOUM¹,
AND MAGDI SADEK MAHMOUD², (Senior Member, IEEE)

¹School of Electrical Engineering, Universiti Teknologi Malaysia, Johor Bahru, Johor 81310, Malaysia

²Systems Engineering Department, King Fahd University of Petroleum and Minerals, Dhahran 31261, Saudi Arabia

Corresponding authors: Ahmed Eltayeb (ahmedtayeb5@gmail.com) and Mohd Fua'ad Rahmat (fuaad@fke.utm.my)

This work was supported in part by the Universiti Teknologi Malaysia High Impact Research under Grant Q.J130000.2451.08G80 and in part by the King Fahd University of Petroleum and Minerals.

ABSTRACT The quadcopter unmanned aerial vehicle (UAV) system is considered a good platform for control scheme design as it is highly nonlinear with coupled dynamics and an under-actuated system. Considering these challenges, this manuscript aimed to propose a control algorithm to control the quadcopter system in the presence of uncertainty and disturbance influences. The integral adaptive sliding mode control scheme has been proposed to control the system. The proposed control scheme is composed of the outer loop controller to control the position of the quadcopter, while the inner loop controls the attitude of the quadcopter. The proposed control law has three major terms, firstly the equivalent control which is developed based on the Lyapunov approach to handle most of the uncertainty and disturbance, secondly the adaptive switching gain, which is achieving fast adaptation against uncertainty, finally the switching function which has been approximated by a tangent hyperbolic function to reduce the unwanted chattering phenomena. The proposed control scheme and its performance have been investigated via a MATLAB/Simulink. The results prove that the implemented control scheme is robust even in the presence of uncertainties and disturbance and the quadcopter tracks the predefined trajectories with limited chattering influence.

INDEX TERMS Quadcopter UAV, integral SMC control, adaptive control, chattering reduction.

I. INTRODUCTION

The quadcopter is a type of unmanned aerial vehicle (UAV). It has some advantages against the other types of UAVs, such as fast maneuverability, easy take-off and landing, and payload capacity. Considering these advantages, the quadcopter UAV can be used to achieve many precise and critical tasks, for instance, military applications, medical applications, agriculture applications, and some other dangerous applications to avoid the risk to the human being.

Prior mentioned applications attract researchers to design robust control algorithms to achieve the assigned tasks precisely. Therefore, this research follows the model-based

The associate editor coordinating the review of this manuscript and approving it for publication was Zhuang Xu¹.

control design approach where the model dynamic is used in the proposed control design phase [1], [2].

The quadcopter is a complex system due to high nonlinearity in the dynamics, unbounded dynamics and uncertainties [3]. Furthermore, the quadcopter often operates in a harsh environment where external disturbance plays a significant role. Therefore, all these challenges must be taken into consideration in the control design stage.

Several advanced control techniques have been developed to control the quadcopter systems in order to handle these challenges. For example, sliding mode control [4], [5], [6], backstepping control [7], [8], feedback linearization [9], [10], adaptive SMC control [11], [12], [13], and high-order sliding mode control [14].

The SMC is classified among the robust nonlinear control algorithm, which provides better performance against

uncertain dynamics and disturbances [11], [15], [16]. Essentially, the SMC composes the equivalent and discontinuous (switching) control terms. The equivalent control deals with the nonlinear system dynamic, whereas the switching control term handles any influences that may occur due to uncertainty and unmodeled dynamics.

The chattering phenomenon is considered a major disadvantage associated with the traditional SMC [17], [18], where the unwanted chattering increases dramatically by increasing the switching gain. Meanwhile, for robust stability against uncertainty, disturbance and unmodeled dynamics, the value of the switching gain must be big enough to guarantee the stability of the quadcopter system.

The unwanted chattering leads to serious issues, for instance, vibration in the mechanical parts of the quadcopter and heat in onboard electronics elements, which results in rapid power loss. This study aims to utilize the SMC control advantages and reduce the impact of the chattering to a satisfactory bound. Some works are reported in the literature and focus on chattering reduction, such as the adaptive SMC control [17], higher-order SMC control [18], and fuzzy gain scheduling SMC [19], [20], [21], [22].

An adaptive SMC has been designed where the switching gain is tuned adaptively following the changes on parameters uncertainties [23], [24]. However, the designed controller was not investigating the chattering influences. An adaptive SMC control law is developed in [25] to achieve fast adaptation and reduce unwanted chattering.

This study proposes a control scheme based on the adaptive SMC control technique. The quadcopter dynamic is divided into two subsystems: position and attitude. Subsequently, an outer loop controller is developed based on the adaptive SMC control technique to control the quadcopter position. An inner loop controller is developed based on the adaptive SMC control technique to control the quadcopter attitude. The overall proposed control scheme provided robust tracking and contributed to chattering reduction.

The developed control law of the proposed adaptive SMC control scheme consists of three major terms, the equivalent term, the switching function and finally, the switching gain. The combination of these three terms contributes to a robust tracking and chattering reduction. Therefore, the contributions of this study are listed as follows:

- The equivalent control term is developed based on Lyapunov approach to handle the bulk of disturbance and uncertainty impact and relieve the burden on the switching control term.
- The switching function (sign(s)) is approximated by hyperbolic function tangent function (tanh(s)) where it contributes to the chattering reduction.
- The switching gain is calculated based on an adaptive formula to achieve fast adaptation against disturbance and uncertainty.

This paper is written in the following pattern. First, section II briefly introduces quadcopter modeling. Then,

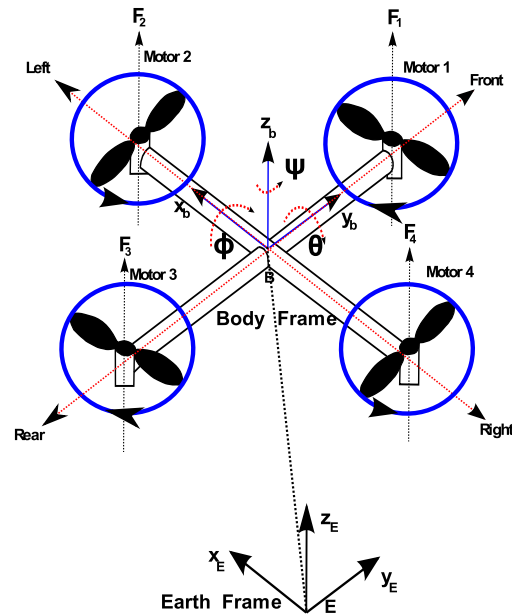


FIGURE 1. Quadcopter configuration [28].

Section III discusses the proposed control scheme. Section IV evaluates the proposed control scheme via the MATLAB/Simulink platform, where the simulation results are presented and discussed. Finally, section V concludes the article.

II. THE QUADCOPTER MODELLING AND DESCRIPTION

In this section, a brief description of the quadcopter has been introduced, then the quadcopter kinematics and the dynamics equations have been presented.

A. QUADCOPTER SYSTEM DESCRIPTION

The quadcopter system composes of four rotors which attached to the mainframe in symmetric cross shape [26], [27], as illustrated in Figure 1.

B. QUADCOPTER KINEMATICS EQUATIONS

To obtain the kinematics equations of the quadcopter, the coordinates space can be given as follows.

$$q = [\xi, \eta]^T \quad (1)$$

where,

$$\xi = [x, y, z]^T \quad (2)$$

and,

$$\eta = [\phi, \theta, \psi]^T \quad (3)$$

Therefore, the translational motion equations of the quadcopter can be written as follows.

$$\dot{\xi} = RV \quad (4)$$

where ξ represents the linear velocity in the E-frame where $E=(x_e, y_e, z_e)$, and V denotes the linear velocity in the B-frame where $B=(x_b, y_b, z_b)$, while R is the transformational matrix (5), as shown at the bottom of the next page.

Similarly, the quadcopter rotational motion equations can be obtained as follows.

$$\dot{\eta} = T\omega \tag{6}$$

where η denotes the angular velocity in the E-frame, and ω denotes the angular velocity in the B-frame. T is the transfer matrix [29], and it's given as follows.

$$T = \begin{bmatrix} 1 & \sin \phi \tan \theta & \cos \phi \tan \theta \\ 0 & \cos \phi & -\sin \phi \\ 0 & \frac{\sin \phi}{\cos \theta} & \frac{\cos \phi}{\cos \theta} \end{bmatrix} \tag{7}$$

C. QUADCOPTER DYNAMIC EQUATIONS

The quadcopter dynamic equations in 6-DOF (space) are presented as follows.

$$\begin{aligned} \ddot{x} &= (\cos \phi \sin \theta \cos \psi + \sin \phi \sin \psi) \frac{u_1}{m} \\ \ddot{y} &= (\cos \phi \sin \theta \sin \psi - \sin \phi \cos \psi) \frac{u_1}{m} \\ \ddot{z} &= -g + (\cos \phi \cos \theta) \frac{u_1}{m} \\ \ddot{\phi} &= a_1 \dot{\theta} \dot{\psi} + a_2 \dot{\theta} \Omega_d + \frac{1}{I_x} u_2 \\ \ddot{\theta} &= a_3 \dot{\phi} \dot{\psi} + a_4 \dot{\phi} \Omega_d + \frac{1}{I_y} u_3 \\ \ddot{\psi} &= a_5 \dot{\phi} \dot{\theta} + \frac{1}{I_z} u_4 \end{aligned} \tag{8}$$

where

$$a_1 = \frac{I_y - I_z}{I_x}, a_2 = \frac{J_r}{I_x}, a_3 = \frac{I_z - I_x}{I_y}, a_4 = \frac{J_r}{I_y},$$

$$\text{and } a_5 = \frac{I_x - I_y}{I_z}$$

and, (u_1, u_2, u_3, u_4) are the control inputs, where

$$\begin{aligned} u_1 &= b(\Omega_1^2 + \Omega_2^2 + \Omega_3^2 + \Omega_4^2) \\ u_2 &= b(\Omega_4^2 - \Omega_2^2) \\ u_3 &= b(\Omega_3^2 - \Omega_1^2) \\ u_4 &= d(\Omega_4^2 + \Omega_2^2 - \Omega_3^2 - \Omega_1^2) \end{aligned} \tag{9}$$

and, Ω_d is written as follows.

$$\Omega_d = -\Omega_1 + \Omega_2 - \Omega_3 + \Omega_4 \tag{10}$$

where the quadcopter model parameters are listed and defined as in Table 1.

III. CONTROL DESIGN

This section discussed the proposed control algorithm design based on the integral adaptive SMC to control the quadcopter attitude and position subsystems, via the inner loop and the outer loop controllers, respectively.

TABLE 1. Model parameters definitions.

Parameter	Definition
m	Mass
I_x	inertia on x-axis
I_y	inertia on y-axis
I_z	inertia on z-axis
b	thrust coefficient
d	drag coefficient
J_r	rotor inertia
l	arm length
Ω	The rotor angular speed

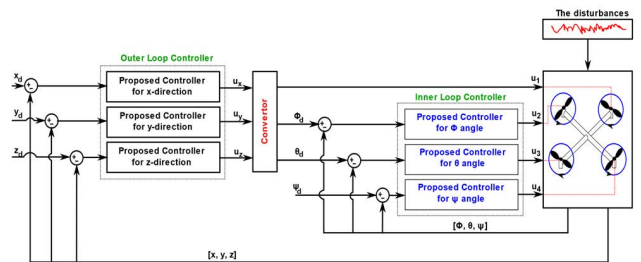


FIGURE 2. Overall proposed control scheme.

A. THE INNER LOOP CONTROLLER DESIGN

The inner loop controller has been proposed based on the integral adaptive SMC to control the quadcopter attitude dynamics, and it is designed based on the following approach.

$$\begin{aligned} \ddot{\phi} &= a_1 \dot{\theta} \dot{\psi} + a_2 \dot{\theta} \Omega_d + \frac{1}{I_x} u_2 + \mu_\phi \\ \ddot{\theta} &= a_3 \dot{\phi} \dot{\psi} + a_4 \dot{\phi} \Omega_d + \frac{1}{I_y} u_3 + \mu_\theta \\ \ddot{\psi} &= a_5 \dot{\phi} \dot{\theta} + \frac{1}{I_z} u_4 + \mu_\psi \end{aligned} \tag{11}$$

where,

$$a_1 = \frac{I_y - I_z}{I_x}, a_2 = \frac{J_r}{I_x}, a_3 = \frac{I_z - I_x}{I_y}, a_4 = \frac{J_r}{I_y},$$

$$\text{and } a_5 = \frac{I_x - I_y}{I_z}$$

and $\mu_\phi, \mu_\theta, \mu_\psi$ denote the external disturbances for ϕ, θ, ψ dynamics, respectively.

The control objective is to develop an integral adaptive SMC control law to stabilize the error dynamics of the quadcopter attitude. The error attitude dynamics are given as follows:

$$\begin{aligned} e_\phi &= \phi - \phi_d \\ e_\theta &= \theta - \theta_d \\ e_\psi &= \psi - \psi_d \end{aligned} \tag{12}$$

$$R = \begin{bmatrix} \cos \theta \cos \psi & \sin \phi \sin \theta \cos \psi & -\cos \phi \cos \psi & \sin \phi \sin \theta \cos \psi & +\cos \phi \sin \psi \\ \cos \theta \sin \psi & \sin \phi \sin \theta \sin \psi & +\cos \phi \cos \psi & \cos \phi \sin \theta \sin \psi & -\sin \phi \cos \psi \\ -\sin \theta & \sin \phi \cos \theta & & \cos \phi \cos \theta & \end{bmatrix} \tag{5}$$

where (ϕ, θ, ψ) is the measured attitude, and $(\phi_d, \theta_d, \psi_d)$ is the reference attitude. The proposed integral adaptive SMC control laws for the attitude have been developed following the below methodology:

Step 1: is to write the dynamics of the errors as in (12).

Step 2: is to select the integral sliding surface as in (13) [5].

$$s = \left(\frac{d}{dt} + k_1 \right)^{n-1} e + k_2 \int_0^t e d\tau \quad (13)$$

Consequently, the integral SMC surface for attitude angles individually is chosen as follows.

$$\begin{aligned} s_\phi &= \dot{e}_\phi + k_{1_\phi} e_\phi + k_{2_\phi} \int_0^t e_\phi d\tau \\ s_\theta &= \dot{e}_\theta + k_{1_\theta} e_\theta + k_{2_\theta} \int_0^t e_\theta d\tau \\ s_\psi &= \dot{e}_\psi + k_{1_\psi} e_\psi + k_{2_\psi} \int_0^t e_\psi d\tau \end{aligned} \quad (14)$$

where, s_ϕ, s_θ and s_ψ represent the integral SMC surfaces. While $k_{1_\phi}, k_{1_\theta}, k_{1_\psi} > 0$ and $k_{2_\phi}, k_{2_\theta}, k_{2_\psi} > 0$ are the inner loop integral SMC control gains.

Step 3: is to implement the sliding mode condition as in the below (15).

$$\dot{s} = -C_1 \text{sgn}(s) - C_2 s \quad (15)$$

where C_1 and C_2 are positive constants.

Substitute (12) into (14), then derivative both sides result to.

$$\begin{aligned} \dot{s}_\phi &= (\ddot{\phi} - \ddot{\phi}_d) + k_{1_\phi} \dot{e}_\phi + k_{2_\phi} e_\phi \\ \dot{s}_\theta &= (\ddot{\theta} - \ddot{\theta}_d) + k_{1_\theta} \dot{e}_\theta + k_{2_\theta} e_\theta \\ \dot{s}_\psi &= (\ddot{\psi} - \ddot{\psi}_d) + k_{1_\psi} \dot{e}_\psi + k_{2_\psi} e_\psi \end{aligned} \quad (16)$$

Substitute (11) into (16), yields to.

$$\begin{aligned} \dot{s}_\phi &= a_1 \dot{\theta} \dot{\psi} + a_2 \dot{\theta} \Omega_d + \frac{1}{I_x} u_2 + \mu_\phi - \ddot{\phi}_d + k_{1_\phi} \dot{e}_\phi + k_{2_\phi} e_\phi \\ \dot{s}_\theta &= a_3 \dot{\phi} \dot{\psi} + a_4 \dot{\phi} \Omega_d + \frac{1}{I_y} u_3 + \mu_\theta - \ddot{\theta}_d + k_{1_\theta} \dot{e}_\theta + k_{2_\theta} e_\theta \\ \dot{s}_\psi &= a_5 \dot{\phi} \dot{\theta} + \frac{1}{I_z} u_4 + \mu_\psi - \ddot{\psi}_d + k_{1_\psi} \dot{e}_\psi + k_{2_\psi} e_\psi \end{aligned} \quad (17)$$

where $k_{1_\phi}, k_{1_\theta}, k_{1_\psi} > 0$ and $k_{2_\phi}, k_{2_\theta}, k_{2_\psi} > 0$ are the design parameters.

Step 4: is to select the control input u_2, u_3, u_4 as follows.

$$u_2 = I_x (\ddot{\phi}_d - a_1 \dot{\theta} \dot{\psi} - a_2 \dot{\theta} \Omega_d - k_{1_\phi} \dot{e}_\phi - k_{2_\phi} e_\phi + \mu_\phi + U_1)$$

$$u_3 = I_y (\ddot{\theta}_d - a_3 \dot{\phi} \dot{\psi} - a_4 \dot{\phi} \Omega_d - k_{1_\theta} \dot{e}_\theta - k_{2_\theta} e_\theta + \mu_\theta + U_2)$$

$$u_4 = I_z (\ddot{\psi}_d - a_5 \dot{\phi} \dot{\theta} - k_{1_\psi} \dot{e}_\psi - k_{2_\psi} e_\psi + \mu_\psi + U_3) \quad (18)$$

Substitute (18) into (17), yields to.

$$\begin{aligned} \dot{s}_\phi &= U_1 + \Gamma_\phi \\ \dot{s}_\theta &= U_2 + \Gamma_\theta \\ \dot{s}_\psi &= U_3 + \Gamma_\psi \end{aligned} \quad (19)$$

where,

$$\begin{aligned} \Gamma_\phi &= I_x \mu_\phi \\ \Gamma_\theta &= I_y \mu_\theta \\ \Gamma_\psi &= I_z \mu_\psi \end{aligned} \quad (20)$$

Step 5: is to calculate the estimated $\Gamma_\phi, \Gamma_\theta, \Gamma_\psi$ based on selected Lyapunov functions as follows.

$$\begin{aligned} V_\phi &= \frac{1}{2} s_\phi^2 + \frac{1}{2} \tilde{\Gamma}_\phi \gamma_\phi \tilde{\Gamma}_\phi \\ V_\theta &= \frac{1}{2} s_\theta^2 + \frac{1}{2} \tilde{\Gamma}_\theta \gamma_\theta \tilde{\Gamma}_\theta \\ V_\psi &= \frac{1}{2} s_\psi^2 + \frac{1}{2} \tilde{\Gamma}_\psi \gamma_\psi \tilde{\Gamma}_\psi \end{aligned} \quad (21)$$

where, $\tilde{\Gamma}_\phi, \tilde{\Gamma}_\theta, \tilde{\Gamma}_\psi$ are errors between the actual and estimated uncertainties which can be written as, $\tilde{\Gamma}_\phi = \Gamma_\phi - \hat{\Gamma}_\phi$, $\tilde{\Gamma}_\theta = \Gamma_\theta - \hat{\Gamma}_\theta$, and $\tilde{\Gamma}_\psi = \Gamma_\psi - \hat{\Gamma}_\psi$, respectively. while $\gamma_\phi, \gamma_\theta$, and γ_ψ are positive constants.

Differentiating the equation (21) leads to.

$$\begin{aligned} \dot{V}_\phi &= s_\phi \dot{s}_\phi + \dot{\tilde{\Gamma}}_\phi \gamma_\phi \tilde{\Gamma}_\phi \\ \dot{V}_\theta &= s_\theta \dot{s}_\theta + \dot{\tilde{\Gamma}}_\theta \gamma_\theta \tilde{\Gamma}_\theta \\ \dot{V}_\psi &= s_\psi \dot{s}_\psi + \dot{\tilde{\Gamma}}_\psi \gamma_\psi \tilde{\Gamma}_\psi \end{aligned} \quad (22)$$

As per (22) the adaption laws are calculated as follows.

$$\begin{aligned} \dot{\hat{\Gamma}}_\phi &= \frac{1}{\gamma_\phi} s_\phi \\ \dot{\hat{\Gamma}}_\theta &= \frac{1}{\gamma_\theta} s_\theta \\ \dot{\hat{\Gamma}}_\psi &= \frac{1}{\gamma_\psi} s_\psi \end{aligned} \quad (23)$$

Therefore, considering (15) and (19), the control laws are obtained as follows.

$$\begin{aligned} U_1 &= -\hat{\Gamma}_\phi - C_{1_\phi} \text{sgn}(s_\phi) - C_{2_\phi} s_\phi \\ U_2 &= -\hat{\Gamma}_\theta - C_{1_\theta} \text{sgn}(s_\theta) - C_{2_\theta} s_\theta \\ U_3 &= -\hat{\Gamma}_\psi - C_{1_\psi} \text{sgn}(s_\psi) - C_{2_\psi} s_\psi \end{aligned} \quad (24)$$

Step 6: to reduce the chattering, the sign(s) is approximated by the hyperbolic function tangent function ($\tanh(s)$). Therefore, the switching function in (24) will be replaced by ($\tanh(s)$), where its formula is given as follows.

$$\tanh(s) = \frac{e^s - e^{-s}}{e^s + e^{-s}} \quad (25)$$

and has properties:

$$\tanh(s) = \begin{cases} 1 & \text{if } s \text{ is a positive big} \\ 0 & \text{if } s = 0, \\ -1 & \text{if } s \text{ is a negative big} \end{cases}$$

Step 7: the switching gains are designed as in (26) to sense and adapt the changes in the uncertainties quickly. There are three parameters φ_i, α_i and $\delta_i(t)$ can be used and selected to

achieve fast adaptation, which contributes to the chattering reduction.

$$\dot{\hat{C}}_i = \begin{cases} \varphi_i \left\{ \alpha_i^{-1} \cdot |s_i(t)| \right\}^{-\delta_i(t)} \cdot \delta_i(t) & \text{if } \hat{C}_i > 0 \\ \varphi_i \cdot \alpha_i^{-1} \cdot |s_i(t)| & \text{if } \hat{C}_i = 0 \end{cases} \quad (26)$$

The parameter φ_i can be tuned as follows:

$$\delta_i(t) = \tanh(\|s_i(t)\|_\infty - \epsilon_i) \quad (27)$$

$$\varphi_i = \begin{cases} \varphi_{i_{up}} & \text{if } \delta_i(t) > 0 \\ \varphi_{i_{down}} & \text{if } \delta_i(t) \leq 0 \end{cases} \quad (28)$$

where, $\varphi_{i_{up}}$ is controlling the increment rate and $\varphi_{i_{down}}$ is controlling the decrement rate.

B. THE OUTER LOOP CONTROLLER DESIG

As it can be observed, the overall dynamics of the quadcopter (attitude and position) as given in (8) are underactuated where there are 6-DOFs $[x, y, z, \phi, \theta, \psi]^T$ controlled via $[u_1, u_2, u_3, u_4]^T$ only [30], [31]. However, as shown in (8), the underactuated part is coming from the quadcopter position dynamics subsystem. Therefore, the Cartesian positions (u_1, ϕ and θ) are utilized to generate three virtual control inputs to control each output individually. Considering the quadcopter position dynamics, the virtual controls can be written as follows.

$$\begin{bmatrix} u_x \\ u_y \\ u_z \end{bmatrix} = \begin{bmatrix} \cos \phi \sin \theta \cos \psi + \sin \phi \sin \psi \\ \cos \phi \sin \theta \sin \psi - \sin \phi \cos \psi \\ \cos \phi \cos \theta \end{bmatrix} \frac{u_1}{m} - \begin{bmatrix} 0 \\ 0 \\ g \end{bmatrix} + \begin{bmatrix} \mu_x \\ \mu_y \\ \mu_z \end{bmatrix} \quad (29)$$

where, μ_x, μ_y and μ_z are the position disturbances.

From (29), the Cartesian positions are calculated as follows.

$$u_1 = \sqrt{u_x^2 + u_y^2 + (u_z + g)^2} \quad (30)$$

and,

$$\phi_d = \sin^{-1} \left(\frac{u_x \sin \psi_d - u_y \cos \psi_d}{u_1} \right) \quad (31)$$

$$\theta_d = \tan^{-1} \left(\frac{u_x \sin \psi_d + u_y \cos \psi_d}{u_z + g} \right) \quad (32)$$

where u_x, u_y and u_z denote the virtual controls generated to control the quadcopter position through (u_1, ϕ_d and θ_d). Particularly, as shown in Figure 2, the outer loop controller takes the errors signals which is the difference between the desired (x_d, y_d, z_d) and the measured (x, y, z) position and produces the virtual controls (u_x, u_y, u_z). Then, the convertor generates the lift force u_1, ϕ_d , and θ_d angles.

The aim of this section is to design an outer loop controller based on the integral adaptive SMC control to stabilize the quadcopter position.

Step 1: Subsequently, the error dynamics of the quadcopter position subsystem are written as follows.

$$\begin{aligned} e_x &= x - x_d \\ e_y &= y - y_d \\ e_z &= z - z_d \end{aligned} \quad (33)$$

Step 2: Similarly, as in the inner loop controller design section, the integral sliding surface for the outer loop controller is written as follows.

$$\begin{aligned} s_x &= \dot{e}_x + k_{1_x} e_x + k_{2_x} \int_0^t e_x d\tau \\ s_y &= \dot{e}_y + k_{1_y} e_y + k_{2_y} \int_0^t e_y d\tau \\ s_z &= \dot{e}_z + k_{1_z} e_z + k_{2_z} \int_0^t e_z d\tau \end{aligned} \quad (34)$$

where, s_x, s_y and s_z represent the sliding surfaces for x, y , and z dynamics, respectively. While $k_{1_x}, k_{1_y}, k_{1_z} > 0$ and $k_{2_x}, k_{2_y}, k_{2_z} > 0$ are the outer loop integral adaptive SMC control gains.

Step 3: is to apply the sliding mode condition as in (15).

$$\begin{aligned} \dot{s}_x &= (\ddot{x} - \ddot{x}_d) + k_{1_x} \dot{e}_x + k_{2_x} e_x \\ \dot{s}_y &= (\ddot{y} - \ddot{y}_d) + k_{1_y} \dot{e}_y + k_{2_y} e_y \\ \dot{s}_z &= (\ddot{z} - \ddot{z}_d) + k_{1_z} \dot{e}_z + k_{2_z} e_z \end{aligned} \quad (35)$$

Then, from (29) and (35), we obtain.

$$\begin{aligned} \dot{s}_x &= u_x + \mu_x - \ddot{x}_d + k_{1_x} \dot{e}_x + k_{2_x} e_x \\ \dot{s}_y &= u_y + \mu_y - \ddot{y}_d + k_{1_y} \dot{e}_y + k_{2_y} e_y \\ \dot{s}_z &= u_z + \mu_z - \ddot{z}_d + k_{1_z} \dot{e}_z + k_{2_z} e_z \end{aligned} \quad (36)$$

Step 4: is to select the control input u_x, u_y, u_z as follows:

$$\begin{aligned} u_x &= \{ \ddot{x}_d - k_{1_x} \dot{e}_x - k_{2_x} e_x \} + U_x \\ u_y &= \{ \ddot{y}_d - k_{1_y} \dot{e}_y - k_{2_y} e_y \} + U_y \\ u_z &= \{ \ddot{z}_d - k_{1_z} \dot{e}_z - k_{2_z} e_z \} + U_z \end{aligned} \quad (37)$$

Therefore, from (36) and (37), we get

$$\begin{aligned} \dot{s}_x &= \mu_x + U_x \\ \dot{s}_y &= \mu_y + U_y \\ \dot{s}_z &= \mu_z + U_z \end{aligned} \quad (38)$$

Thus,

$$\begin{aligned} \dot{s}_x &= U_x + \Gamma_x \\ \dot{s}_y &= U_y + \Gamma_y \\ \dot{s}_z &= U_z + \Gamma_z \end{aligned} \quad (39)$$

where,

$$\begin{aligned} \Gamma_x &= \mu_x \\ \Gamma_y &= \mu_y \\ \Gamma_z &= \mu_z \end{aligned} \quad (40)$$

TABLE 2. The quadcopter model Parameters [32].

Name	Parameter	Value	Unit
Mass	m	65×10^{-2}	kg
inertia on x-axis	I_x	75×10^{-4}	kgm ²
inertia on y-axis	I_y	75×10^{-4}	kgm ²
inertia on z-axis	I_z	13×10^{-3}	kgm ²
thrust coefficient	b	313×10^{-6}	Ns ²
drag coefficient	d	7.5×10^{-7}	Nms ²
rotor inertia	J_r	6×10^{-5}	kgm ²
arm length	l	23×10^{-2}	m

Step 5: is to calculate the estimated $\Gamma_x, \Gamma_y, \Gamma_z$ based on selected Lyapunov functions as follows.

$$\begin{aligned}
 V_x &= \frac{1}{2}s_x^2 + \frac{1}{2}\tilde{\Gamma}_x\gamma_x\tilde{\Gamma}_x \\
 V_y &= \frac{1}{2}s_y^2 + \frac{1}{2}\tilde{\Gamma}_y\gamma_y\tilde{\Gamma}_y \\
 V_z &= \frac{1}{2}s_z^2 + \frac{1}{2}\tilde{\Gamma}_z\gamma_z\tilde{\Gamma}_z
 \end{aligned} \tag{41}$$

where, $\tilde{\Gamma}_x, \tilde{\Gamma}_y, \tilde{\Gamma}_z$ are the uncertainty errors, and calculated as $\tilde{\Gamma}_x = \Gamma_x - \hat{\Gamma}_x, \tilde{\Gamma}_y = \Gamma_y - \hat{\Gamma}_y,$ and $\tilde{\Gamma}_z = \Gamma_z - \hat{\Gamma}_z,$ while, $\gamma_x, \gamma_y,$ and γ_z are positive constants.

Therefore, the first derivative for both sides of the selected Lyapunov function (41) yields to.

$$\begin{aligned}
 \dot{V}_x &= s_x\dot{s}_x + \dot{\tilde{\Gamma}}_x\gamma_x\tilde{\Gamma}_x \\
 \dot{V}_y &= s_y\dot{s}_y + \dot{\tilde{\Gamma}}_y\gamma_y\tilde{\Gamma}_y \\
 \dot{V}_z &= s_z\dot{s}_z + \dot{\tilde{\Gamma}}_z\gamma_z\tilde{\Gamma}_z
 \end{aligned} \tag{42}$$

The adaption laws are calculated as follows.

$$\begin{aligned}
 \dot{\hat{\Gamma}}_x &= \frac{1}{\gamma_x}s_x \\
 \dot{\hat{\Gamma}}_y &= \frac{1}{\gamma_y}s_y \\
 \dot{\hat{\Gamma}}_z &= \frac{1}{\gamma_z}s_z
 \end{aligned} \tag{43}$$

Thus, the control laws will be as follows.

$$\begin{aligned}
 U_x &= -\hat{\Gamma}_x - C_{1_x}sgn(s_x) - C_{2_x}s_x \\
 U_y &= -\hat{\Gamma}_y - C_{1_y}sgn(s_y) - C_{2_y}s_y \\
 U_z &= -\hat{\Gamma}_z - C_{1_z}sgn(s_z) - C_{2_z}s_z
 \end{aligned} \tag{44}$$

To reduce the chattering, steps 6 and 7 are implemented as in the previous section.

IV. SIMULATION MODEL

The proposed control scheme has been simulated and evaluated via the MATLAB/Simulink platform. The designed control parameters are listed in Table 3 and Table 4 for the inner and the outer loop controllers, respectively.

TABLE 3. The inner loop Controller parameters for the attitude.

Parameters	ϕ	θ	ψ
$C_{2_{\phi,\theta,\psi}}$	0.8	0.8	0.8
$\gamma_{\phi,\theta,\psi}$	5	5	5
$\varepsilon_{\phi,\theta,\psi}$	0.005	0.01	0.02
$\varphi_{up_{\phi,\theta,\psi}}$	0.6	0.8	0.4
$\varphi_{down_{\phi,\theta,\psi}}$	5	8	2
$\alpha_{\phi,\theta,\psi}$	50	50	1

TABLE 4. The outer loop Controller parameters for the position.

Parameters	x	y	z
$C_{2_{x,y,z}}$	0.8	0.8	0.8
$\gamma_{x,y,z}$	5	5	5
$\varepsilon_{x,y,z}$	0.005	0.01	0.02
$\varphi_{up_{x,y,z}}$	0.6	0.8	0.4
$\varphi_{down_{x,y,z}}$	5	8	2
$\alpha_{x,y,z}$	50	50	1

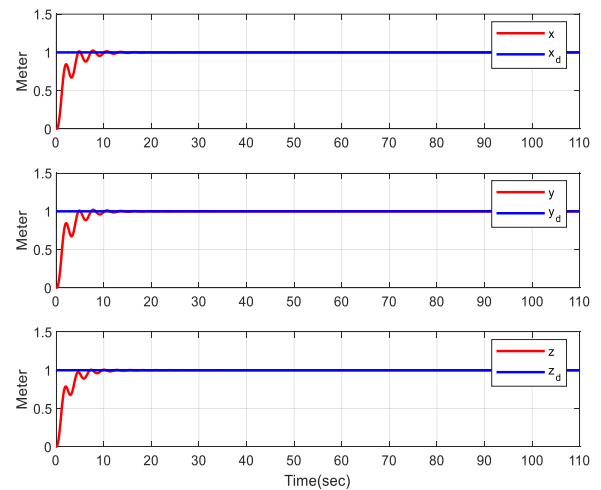


FIGURE 3. Quadcopter position-following the desired position in space.

V. SIMULATION RESULTS

To evaluate the performance of the proposed control scheme, three different scenarios have been investigated. In the first case, the quadcopter has been commanded to reach the desired position. In the second case, the quadcopter has been commanded to track a predefined reference trajectory. Finally, the proposed control scheme has been evaluated, considering both the external disturbance and the quadcopter mass uncertainty, where the quadcopter is following the predefined track.

A. CONTROL SYSTEM PERFORMANCE: ACHIEVING THE DESIRED POSITION

In this scenario, the desired setpoint in space is defined as $(x_d, y_d, z_d),$ and the quadcopter UAV has been commanded to reach that point. The proposed control scheme is designed to achieve the assigned task precisely and fastly as shown in Figure 3 and Figure 4 for the position

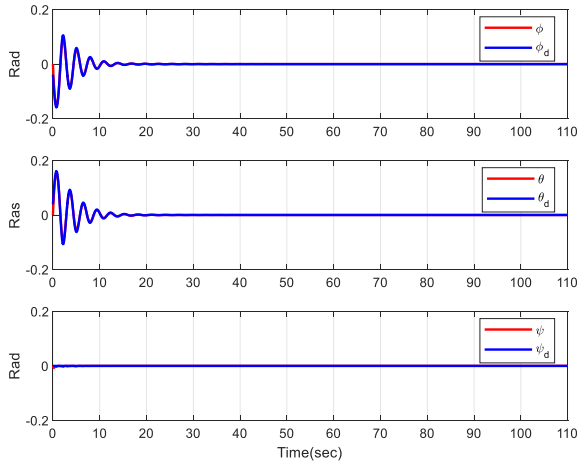


FIGURE 4. Quadcopter attitude-following the desired angles in space.

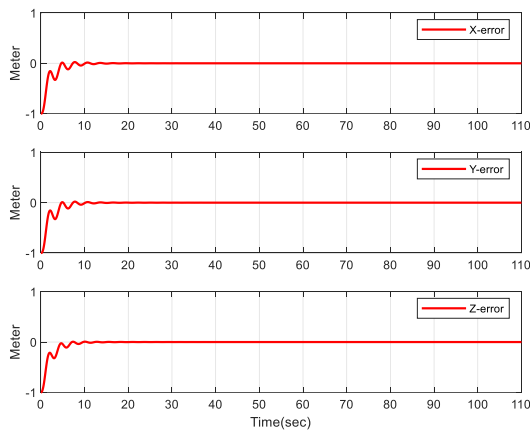


FIGURE 5. Quadcopter position errors signals.

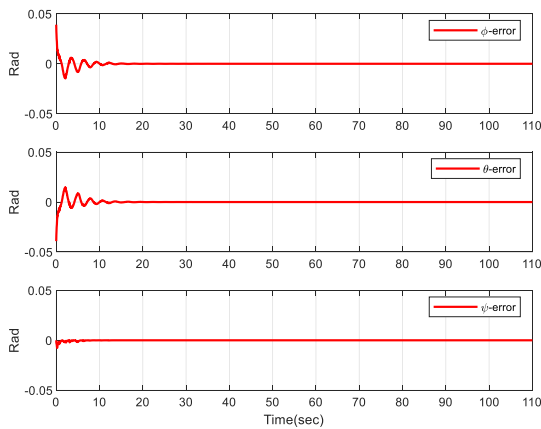


FIGURE 6. Quadcopter attitude errors signals.

and attitude, respectively. Figure 5 and Figure 6 presented the associated errors for the position and attitude, respectively. Figure 7 presents the control efforts to accomplish the assigned tasks.

B. CONTROL SYSTEM PERFORMANCE: FOLLOWING REFERENCE TRAJECTORY TRACKING

In this case, the quadcopter is simulated and commanded to track a predefined trajectory in space 6-DOFs (for the position as in Figure 8 and Figure 9, and for the attitude as in

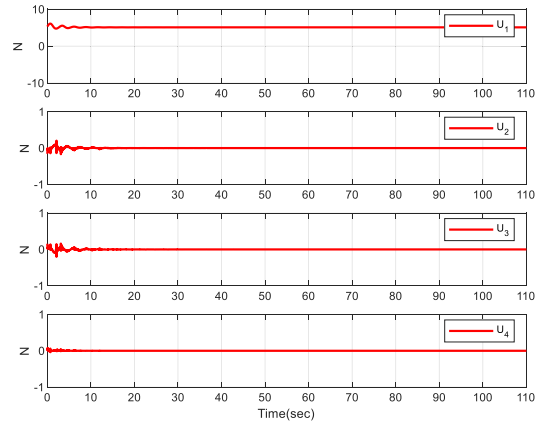


FIGURE 7. Quadcopter control signals.

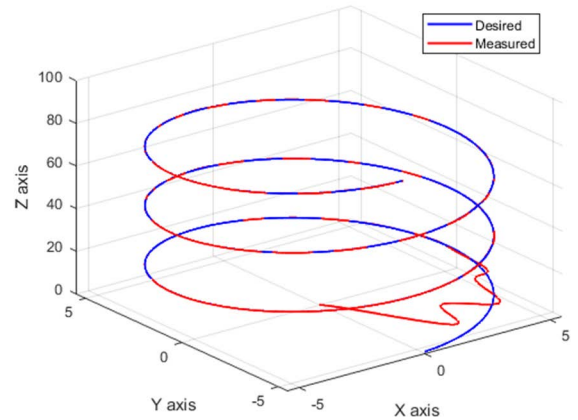


FIGURE 8. 3D view of desired trajectory tracking- nominal parameters.

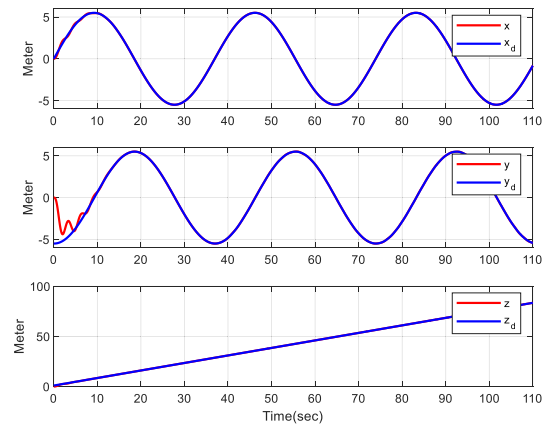


FIGURE 9. Quadcopter position-following the desired position in space-nominal parameters.

Figure 10), considering the ideal environment where there is no influence neither from the uncertainties nor disturbances. This scenario is almost similar and applicable for indoor quadcopter applications where the operation area is limited and closed.

The simulation results in this scenario prove that the proposed controller is robust against the reference tracking modification. In the previous scenario, the performance was evaluated for the quadcopter to reach the reference setpoint, whereas, in this scenario, the proposed controller is evaluated

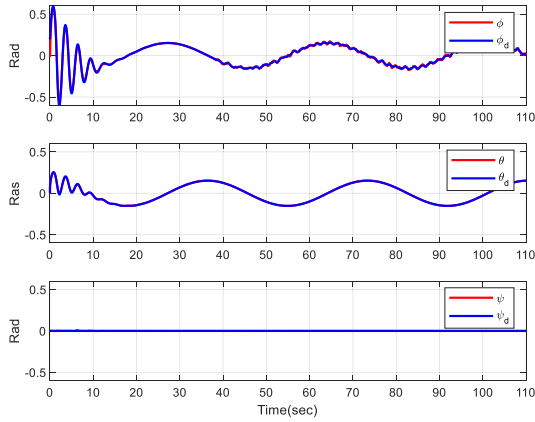


FIGURE 10. Quadcopter attitude-following the desired angles in space-nominal parameters.

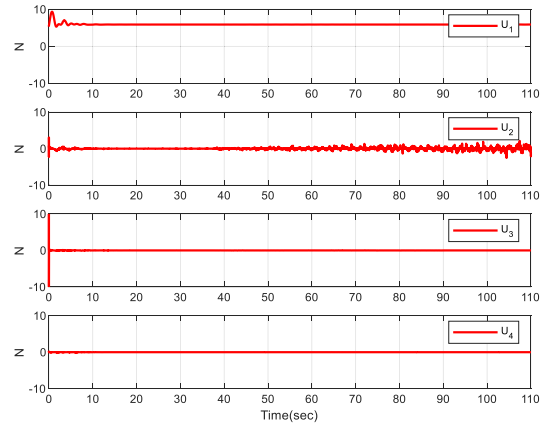


FIGURE 13. Quadcopter control signals-nominal parameters.

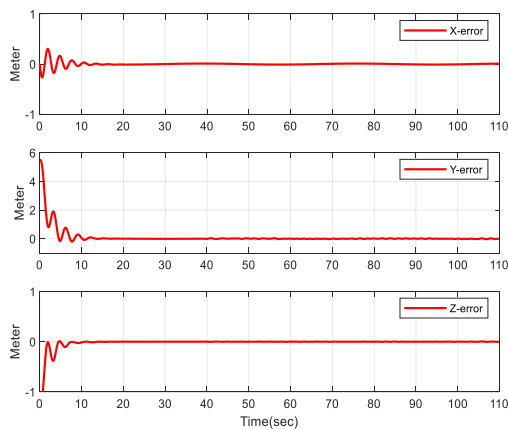


FIGURE 11. Quadcopter position errors signals (nominal parameters).

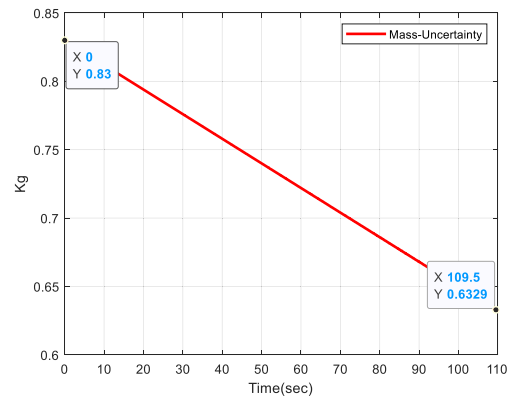


FIGURE 14. Quadcopter variable payloads (mass uncertainty).

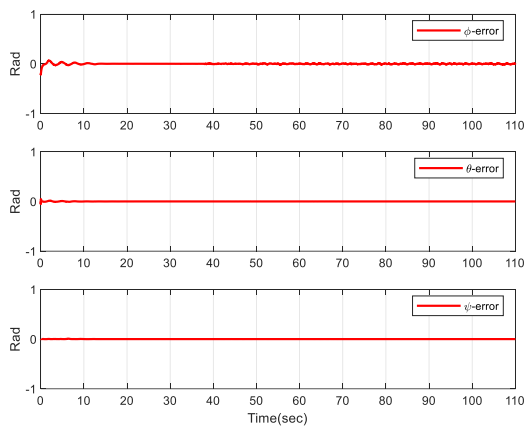


FIGURE 12. Quadcopter attitude errors signals-nominal parameters.

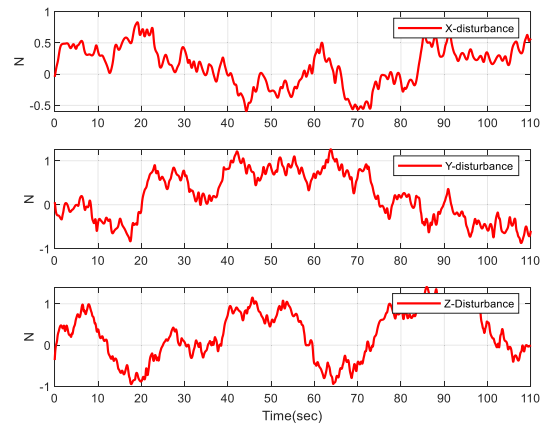


FIGURE 15. External disturbances acting on x, y and z-axes.

to follow a full predefined trajectory tracking in space. Figure 11 and Figure 12 visualize the error signals for the position and attitude, respectively. The control efforts that enabled the quadcopter to achieve this task successfully are shown in Figure 13.

C. THE CONTROL SYSTEM PERFORMANCE: FOLLOWING REFERENCE TRAJECTORY TRACKING AGAINST THE VARIABLE PAYLOAD AND DISTURBANCE

In this scenario, the quadcopter is simulated to mimic the real and harsh environment applicable in some outdoor

applications such as spraying agricultural pesticides where the disturbances and uncertainties are challenging. In this case the uncertainty has been represented by a variable payload where it is assumed as an added mass (such as liquid pesticides) 0.18 kg to the quadcopter nominal mass 0.65 kg; the added mass is about 30%. As shown in Figure 14 the added mass discharges linearly until the liquid pesticides finish and the quadcopter mass returns to the nominal value. Meanwhile, the disturbances have been considered as well as depicted in Figure 15.

Despite these challenges, the proposed controller still enables the quadcopter to track a predefined trajectory in

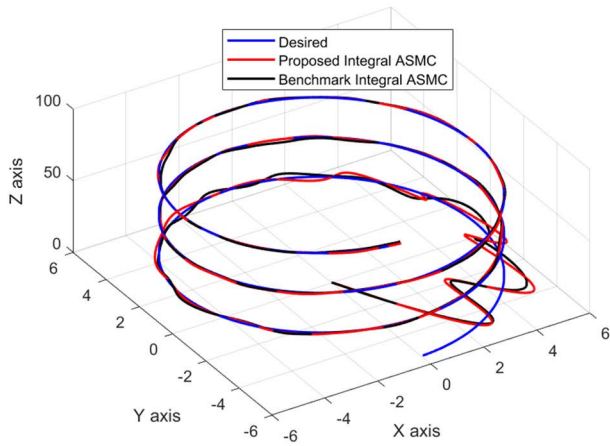


FIGURE 16. 3D view of desired trajectory tracking in the presence of disturbance and mass uncertainty.

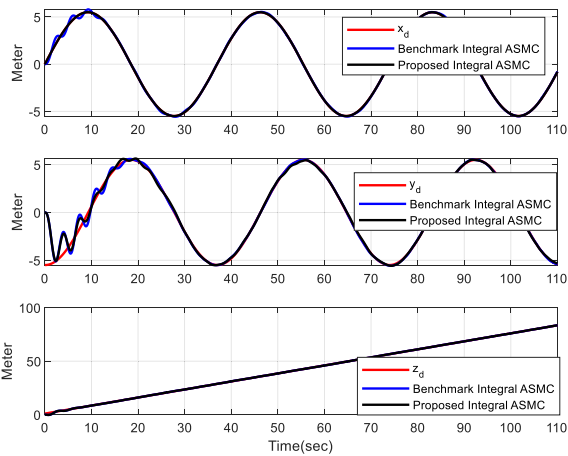


FIGURE 17. Quadcopter position-following the desired position in space-in the presence of disturbance and mass uncertainty.

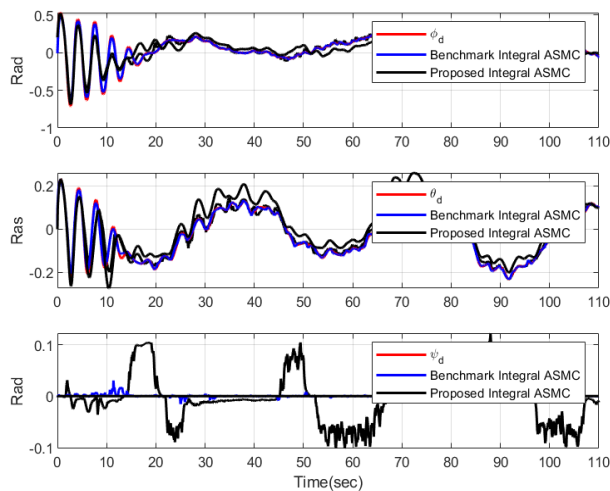


FIGURE 18. Quadcopter attitude-following the desired angles in space-in the presence of disturbance and mass uncertainty.

space 6-DOFs for (the position as in Figure 16 for 3D view and Figure 17 and the attitude as in Figure 18). The assigned task has been achieved successfully, and the controller performance can be observed as in Figure 19, and

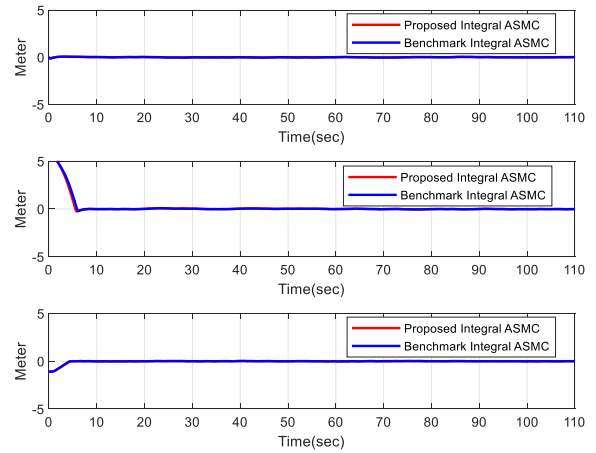


FIGURE 19. Quadcopter position errors signals-in the presence of disturbance and mass uncertainty.

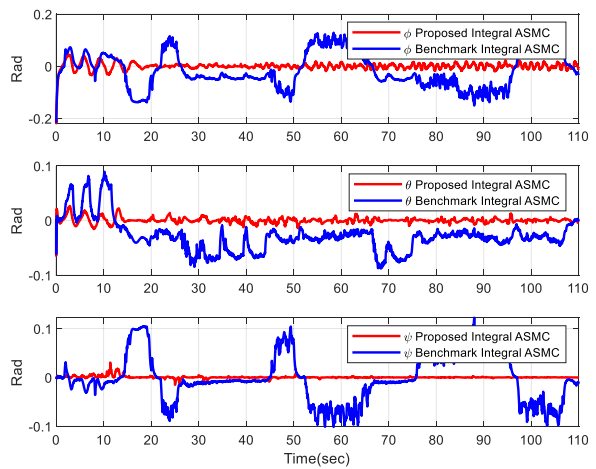


FIGURE 20. Quadcopter attitude errors signals-in the presence of disturbance and mass uncertainty.

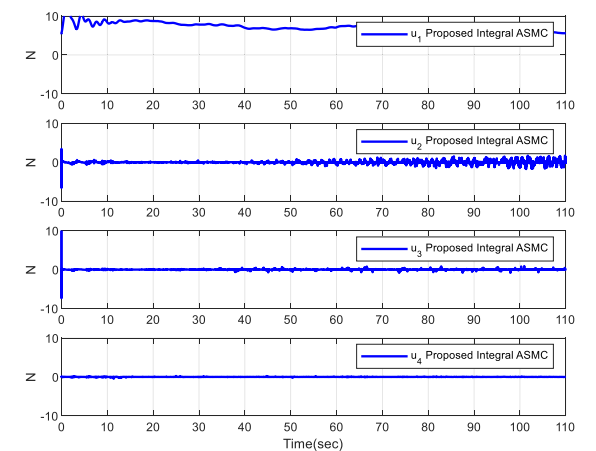


FIGURE 21. Quadcopter control signals- in the presence of disturbance and mass uncertainty.

Figure 20, which presented the errors in quadcopter position and attitude, respectively. The control efforts that enabled the quadcopter to overcome these challenges with satisfactory chattering as shown in Figure 21. The performance of

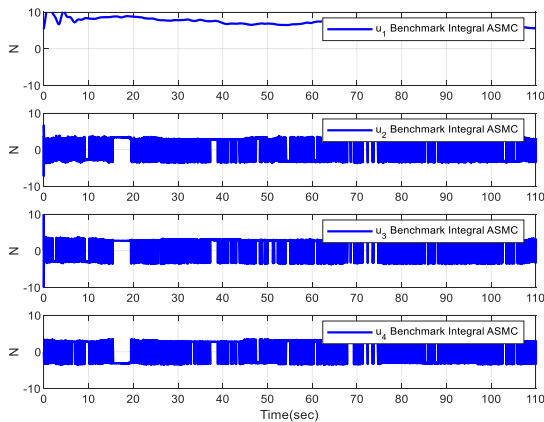


FIGURE 22. Quadcopter control signals- in the presence of disturbance and mass uncertainty.

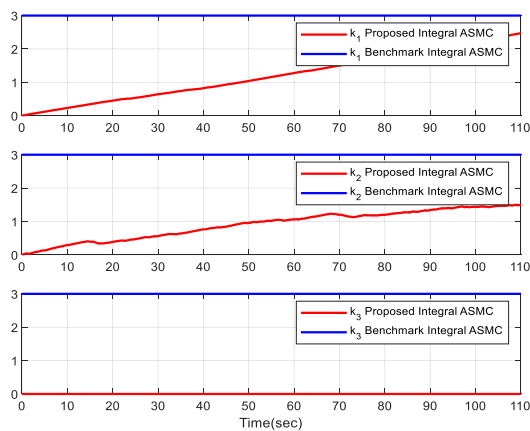


FIGURE 23. Adaptive estimated gains vs the constant gains.

the proposed control scheme has been compared with the benchmark integral adaptive SMC controller in which the gain is considered as constant and the switching function is considered as $\text{sign}(s)$ without an approximation to study and investigate the performance of the proposed integral adaptive SMC control scheme in terms of the chattering attenuation and robustness. The results have been shown in Figure 21 and Figure 22 which represent the performance of the proposed controller and benchmark controller, respectively, where the performance of the proposed controller outperformed the benchmark controller. While Figure 23 visualizes the behavior of the adaptive gains against the uncertainties and the disturbance.

VI. CONCLUSION

In this paper, the proposed control scheme has been developed based on the adaptive SMC control algorithm. The quadcopter dynamic is divided into two parts, the position and the attitude subsystems. Subsequently, an outer loop controller has been designed based on the adaptive SMC control method to control the quadcopter position. Also, an inner loop controller has been developed based on the adaptive SMC control technique to control the quadcopter attitude. The overall proposed control scheme provided robust tracking and

contributed to chattering reduction. Based on the proposed integral SMC, it is suggested to proceed further to identify the unknown dynamics, which is also important for UAV control. Currently, intelligent algorithms are widely used in online estimation, e.g., neuroadaptive control for complicated underactuated systems with simultaneous output and velocity constraints; adaptive fuzzy control for a class of MIMO underactuated systems with plant uncertainties and actuator dead-zones. These topics are the subject of future research.

REFERENCES

- [1] W. Gu, K. P. Valavanis, M. J. Rutherford, and A. Rizzo, "UAV model-based flight control with artificial neural networks: A survey," *J. Intell. Robot. Syst.*, vol. 100, nos. 3–4, pp. 1469–1491, Dec. 2020, doi: [10.1007/s10846-020-01227-8](https://doi.org/10.1007/s10846-020-01227-8).
- [2] A. Taleizadeh, E. Najafi, H. N. Pishkenari, and A. Alasty, "Deployment of model-based design approach for a mini-quadcopter," in *Proc. 7th Int. Conf. Robot. Mechatronics (ICRoM)*, Nov. 2019, pp. 291–296, doi: [10.1109/ICRoM48714.2019.9071917](https://doi.org/10.1109/ICRoM48714.2019.9071917).
- [3] I. S. Leal, C. Abeykoon, and Y. S. Perera, "Design, simulation, analysis and optimization of PID and fuzzy based control systems for a quadcopter," *Electronics*, vol. 10, no. 18, p. 2218, Sep. 2021, doi: [10.3390/electronics10182218](https://doi.org/10.3390/electronics10182218).
- [4] Y. Shtessel, C. Edwards, L. Fridman, and A. Levant, *Sliding Mode Control and Observation*. New York, NY, USA: Springer, 2014.
- [5] S. Vaidyanathan and C. H. Lien, *Applications of Sliding Mode Control in Science and Engineering*, vol. 709. Cham, Switzerland: Springer, 2017.
- [6] A. Noordin, M. A. M. Basri, and Z. Mohamed, "Sliding mode control for altitude and attitude stabilization of quadrotor UAV with external disturbance," *Indonesian J. Elect. Eng. Inform.*, vol. 7, no. 2, pp. 203–210, 2019, doi: [10.11591/ijeei.v7i2.1149](https://doi.org/10.11591/ijeei.v7i2.1149).
- [7] A. T. Nguyen, N. Xuan-Mung, and S. K. Hong, "Quadcopter adaptive trajectory tracking control: A new approach via backstepping technique," *Appl. Sci.*, vol. 9, no. 18, pp. 1–17, 2019, doi: [10.3390/app9183873](https://doi.org/10.3390/app9183873).
- [8] M. A. M. Basri, "Robust backstepping controller design with a fuzzy compensator for autonomous hovering quadrotor UAV," *Iranian J. Sci. Technol., Trans. Electr. Eng.*, vol. 42, no. 3, pp. 379–391, Sep. 2018, doi: [10.1007/s40998-018-0080-6](https://doi.org/10.1007/s40998-018-0080-6).
- [9] E. Kuantama, I. Tarca, and R. Tarca, "Feedback linearization LQR control for quadcopter position tracking," in *Proc. 5th Int. Conf. Control, Decis. Inf. Technol. (CoDIT)*, Apr. 2018, pp. 204–209, doi: [10.1109/CoDIT.2018.8394911](https://doi.org/10.1109/CoDIT.2018.8394911).
- [10] J. C. Escobar, R. Lozano, and M. B. Estrada, "PVTOL control using feedback linearisation with dynamic extension," *Int. J. Control*, vol. 94, no. 7, pp. 1794–1803, Jul. 2021, doi: [10.1080/00207179.2019.1676468](https://doi.org/10.1080/00207179.2019.1676468).
- [11] O. Mofid and S. Mobayen, "Adaptive sliding mode control for finite-time stability of quad-rotor UAVs with parametric uncertainties," *ISA Trans.*, vol. 72, pp. 1–14, Jan. 2018, doi: [10.1016/j.isatra.2017.11.010](https://doi.org/10.1016/j.isatra.2017.11.010).
- [12] S. Nadda and A. Swarup, "On adaptive sliding mode control for improved quadrotor tracking," *J. Vib. Control*, vol. 24, no. 14, pp. 3219–3230, Jul. 2018, doi: [10.1177/1077546317703541](https://doi.org/10.1177/1077546317703541).
- [13] D. Lee, H. J. Kim, and S. Sastry, "Feedback linearization vs. adaptive sliding mode control for a quadrotor helicopter," *Int. J. Control, Autom., Syst.*, vol. 7, no. 3, pp. 419–428, 2009, doi: [10.1007/s12555-009-0311-8](https://doi.org/10.1007/s12555-009-0311-8).
- [14] L. Liu, W. X. Zheng, and S. Ding, "High-order sliding mode controller design subject to lower-triangular nonlinearity and its application to robotic system," *J. Franklin Inst.*, vol. 357, no. 15, pp. 10367–10386, Oct. 2020, doi: [10.1016/j.jfranklin.2020.08.013](https://doi.org/10.1016/j.jfranklin.2020.08.013).
- [15] A. Mazinan, M. Kazemi, and H. Shirzad, "An efficient robust adaptive sliding mode control approach with its application to secure communications in the presence of uncertainties, external disturbance and unknown parameters," *Trans. Inst. Meas. Control*, vol. 36, no. 2, pp. 164–174, Apr. 2014, doi: [10.1177/0142331213492544](https://doi.org/10.1177/0142331213492544).
- [16] J. Zhu and K. Khayati, "A new approach for adaptive sliding mode control: Integral/exponential gain law," *Trans. Inst. Meas. Control*, vol. 38, no. 4, pp. 385–394, Apr. 2016, doi: [10.1177/0142331215583328](https://doi.org/10.1177/0142331215583328).
- [17] O. Barambones and P. Alkorta, "Position control of the induction motor using an adaptive sliding-mode controller and observers," *IEEE Trans. Ind. Electron.*, vol. 61, no. 12, pp. 6556–6565, Dec. 2014, doi: [10.1109/TIE.2014.2316239](https://doi.org/10.1109/TIE.2014.2316239).

- [18] S. Di Gennaro, J. R. Domínguez, and M. A. Meza, "Sensorless high order sliding mode control of induction motors with core loss," *IEEE Trans. Ind. Electron.*, vol. 61, no. 6, pp. 2678–2689, Jun. 2014, doi: [10.1109/TIE.2013.2276311](https://doi.org/10.1109/TIE.2013.2276311).
- [19] A. Eltayeb, M. F. Rahmat, M. A. M. Eltoum, and M. A. M. Basri, "Adaptive fuzzy gain scheduling sliding mode control for quadrotor UAV systems," in *Proc. 8th Int. Conf. Modeling Simulation Appl. Optim. (ICMSAO)*, Apr. 2019, pp. 1–5, doi: [10.1109/ICMSAO.2019.8880438](https://doi.org/10.1109/ICMSAO.2019.8880438).
- [20] Y. Yang and Y. Yan, "Attitude regulation for unmanned quadrotors using adaptive fuzzy gain-scheduling sliding mode control," *Aerosp. Sci. Technol.*, vol. 54, pp. 208–217, Jul. 2016, doi: [10.1016/j.ast.2016.04.005](https://doi.org/10.1016/j.ast.2016.04.005).
- [21] N. Ben, S. Bouallègue, and J. Haggège, "Fuzzy gains-scheduling of an integral sliding mode controller for a quadrotor unmanned aerial vehicle," *Int. J. Adv. Comput. Sci. Appl.*, vol. 9, no. 3, pp. 132–141, 2018, doi: [10.14569/ijacsa.2018.090320](https://doi.org/10.14569/ijacsa.2018.090320).
- [22] E. Ahmed, "Robust adaptive sliding mode control design for quadrotor unmanned aerial vehicle trajectory tracking," *Int. J. Comput. Digit. Syst.*, vol. 9, no. 2, pp. 249–257, Jan. 2020, doi: [10.12785/IJCDS/090210](https://doi.org/10.12785/IJCDS/090210).
- [23] M. M. Rezaei and J. Soltani, "Robust control of an islanded multi-bus microgrid based on input-output feedback linearisation and sliding mode control," *IET Gener., Transmiss. Distrib.*, vol. 9, no. 15, pp. 2447–2454, Nov. 2015, doi: [10.1049/iet-gtd.2015.0340](https://doi.org/10.1049/iet-gtd.2015.0340).
- [24] A. Eltayeb, M. F. Rahmat, M. A. M. Eltoum, S. Ibrahim, and M. A. M. Basri, "Adaptive sliding mode control design for the 2-DOF robot arm manipulators," in *Proc. Int. Conf. Comput., Control, Electr., Electron. Eng. (ICCCEEE)*, Sep. 2019, pp. 1–5, doi: [10.1109/ICCCEEE46830.2019.9071314](https://doi.org/10.1109/ICCCEEE46830.2019.9071314).
- [25] J. Baek, M. Jin, and S. Han, "A new adaptive sliding-mode control scheme for application to robot manipulators," *IEEE Trans. Ind. Electron.*, vol. 63, no. 6, pp. 3628–3637, Jun. 2016, doi: [10.1109/TIE.2016.2522386](https://doi.org/10.1109/TIE.2016.2522386).
- [26] Q. Quan, *Introduction to Multicopter Design and Control*. Beijing, China: Springer, 2017.
- [27] A. Eltayeb, M. F. Rahmat, and M. A. M. Basri, "Adaptive feedback linearization controller for stabilization of quadrotor UAV," *Int. J. Integr. Eng.*, vol. 12, no. 4, pp. 1–17, 2020, doi: [10.30880/ijie.2020.12.04.001](https://doi.org/10.30880/ijie.2020.12.04.001).
- [28] A. Eltayeb, M. F. Rahmat, M. A. M. Basri, and M. S. Mahmoud, "An improved design of integral sliding mode controller for chattering attenuation and trajectory tracking of the quadrotor UAV," *Arabian J. Sci. Eng.*, vol. 45, no. 8, pp. 6949–6961, Aug. 2020, doi: [10.1007/s13369-020-04569-5](https://doi.org/10.1007/s13369-020-04569-5).
- [29] R. Olfati-Saber, "Nonlinear control of underactuated mechanical systems with application to robotics and aerospace vehicles," Ph.D. Thesis, Massachusetts Inst. Technol., Cambridge, MA, USA, 2001.
- [30] H. Boudjedir, O. Bouhali, and N. Rizoug, "Adaptive neural network control based on neural observer for quadrotor unmanned aerial vehicle," *Adv. Robot.*, vol. 28, no. 17, pp. 1151–1164, Sep. 2014, doi: [10.1080/01691864.2014.913498](https://doi.org/10.1080/01691864.2014.913498).
- [31] Z. Li, X. Ma, and Y. Li, "Model-free control of a quadrotor using adaptive proportional derivative-sliding mode control and robust integral of the signum of the error," *Int. J. Adv. Robot. Syst.*, vol. 15, no. 5, pp. 1–15, 2018, doi: [10.1177/1729881418800885](https://doi.org/10.1177/1729881418800885).
- [32] S. Bouabdallah, "Design and control of quadrotors with application to autonomous flying," Ph.D. thesis, Lausanne, EPFL, Laboratoire de Systèmes Autonomes, 2007.



AHMED ELTAYEB received the B.S. degree in electronic engineering from the University of Gezira, Sudan, in 2008, and the M.Sc. degree in systems engineering from the King Fahd University of Petroleum and Minerals, Saudi Arabia, in 2013. He is currently pursuing the Ph.D. degree with the Division of Control and Mechatronics Engineering, UTM University, Malaysia. He was appointed as a Teaching Assistant at the Department of Electronic Engineering, University of Gezira, from 2008 to 2010. He was appointed as a Researcher Assistant at the Department of Systems Engineering, KFUPM University. His research interests include robotics and unmanned aerial vehicles control design.



MOHD FUA'AD RAHMAT (Senior Member, IEEE) received the B.E.Eng. (Hons.) from Universiti Teknologi Malaysia (UTM), Skudai Johor, in 1989, the master's degree in control system engineering from The University of Sheffield, U.K., in 1993, and the Ph.D. degree in electronic instrumentation engineering from Sheffield Hallam University, U.K., in 1996. He is currently a Professor with the Department of Control and Mechatronics Engineering, Faculty of Electrical Engineering, UTM. His research interests include system identification and estimation, signal processing, process tomography for industrial process, process control instrumentation, sensors and actuators, hydraulic, and pneumatic systems.



MOHD ARIFFANAN MOHD BASRI received the B.Eng. degree in electrical and mechatronics, the M.Eng. degree in electrical and mechatronics and automatic control, and the Ph.D. degree in electrical and control degree from Universiti Teknologi Malaysia (UTM), Johor Bahru, Malaysia, in 2004, 2009, and 2015, respectively. He is currently a Senior Lecturer with the School of Electrical Engineering, Faculty of Engineering, UTM. He has authored over 30 journal and conference papers, and book chapters. His current research interests include advanced control techniques, artificial intelligent, and their applications. He is a member of the Board of Engineers Malaysia (BEM), the Malaysia Board of Technologists (MBOT), the Malaysian Society for Automatic Control Engineers (MACE), the Malaysian Simulation Society (MSS), and the International Association of Engineers (IAENG).



M. A. MOHAMMED ELTOUM received the B.S. degree in electrical engineering from the Sudan University of Science and Technology, Sudan, in 2015, and the master's degree in systems and control engineering from the King Fahd University of Petroleum and Minerals, Saudi Arabia, in 2020. He is currently pursuing the Ph.D. degree with Khalifa University, UAE. His research interests include nonlinear control systems, electric drives, mechatronics, and intelligent control systems.



MAGDI SADEK MAHMOUD (Senior Member, IEEE) is a Distinguished Professor at the King Fahd University of Petroleum and Minerals (KFUPM), Saudi Arabia. He was on the faculty at different universities worldwide including Egypt (CU, AUC), Kuwait (KU), UAE (UAU), U.K. (UMIST), USA (Pitt, Case Western), Singapore (Nanyang), and Australia (Adelaide). He lectured in Venezuela (Caracas), Germany (Hanover), U.K. (Kent), USA (UoSA), Canada (Montreal), and China (BIT, Yanshan). He is the principal author of fifty-one (51) books, inclusive book chapters and the author/co-author of more than 610 peer-reviewed articles. He is a fellow of the IEE, the CEI (UK), and a registered consultant engineer of information engineering and systems (Egypt). He has received several national, regional, and international prizes in recognition of his outstanding research. He has served on the Editorial Board of several International Journals. He is currently actively engaged in teaching and research in the development of modern methodologies to distributed control and filtering, networked control systems, fault-tolerant systems, cyberphysical systems, and information technology.

• • •